

## ARGO-YBJ experiment: the Scaler Mode Technique

Irina James\* on behalf of ARGO-YBJ collaboration

*Department of Nuclear and Theoretical Physics, Pavia University,  
27100 Pavia, Italy*

*\* E-mail: [irina.james@pv.infn.it](mailto:irina.james@pv.infn.it)  
<http://argo.na.infn.it>*

The ARGO-YBJ detector is an Extensive Air Shower (EAS) array located in Tibet (P.R. China) at 4300 m a.s.l., performing a continuous sky observation by shower reconstruction with an energy threshold of a few hundreds of GeV. To lower this energy threshold to  $E \sim 1$  GeV the detector has been designed to work in scaler mode, i.e. recording the counting rate of each module of the detector at fixed time intervals. At these energies, signals due to local (e.g. solar events) and cosmological (e.g. Gamma Ray Bursts, GRBs) phenomena are expected as a significant enhancement of the counting rate over the background. Results on the search for GRBs in coincidence with satellite detections are presented.

*Keywords:* Cosmic Rays, Gamma Ray Bursts, Resistive Plate Chambers, Extensive Air Showers

### 1. Introduction

Emission from GRBs in the GeV-TeV energy range has been predicted theoretically and the possible detection of this high energy component plays an important role in constraining different emission models. Emission above 1 GeV has been reported for 3 GRBs, with one photon reaching 18 GeV [1], proving that the spectra of at least some GRBs extend to the GeV energy range. The ARGO-YBJ experiment, thanks to the large field of view ( $> 4$  sr, limited only by the geometrical acceptance), the high duty cycle and the low energy threshold (especially in scaler mode), is particularly suitable to search for these transient phenomena.

### 2. The detector

The detector consists of a single layer of Resistive Plate Chambers (RPC) operating in streamer mode and has a modular structure, the basic module being the cluster ( $5.7 \times 7.6$  m<sup>2</sup>) (see [2] and references quoted therein, for

a complete apparatus description). The whole carpet will be made of 154 clusters, of which 130 are in data taking, with a detection area of  $\sim 6700 \text{ m}^2$  and  $\sim 93\%$  of active area. The detector is connected to two different DAQs, corresponding to two operation modes: the shower and the scaler modes. In shower mode, for each event the location and timing of the secondary particles is recorded, allowing the reconstruction of the lateral distribution and the arrival direction with a threshold energy of a few hundreds of GeV. The lower limit of the detector ( $E \sim 1 \text{ GeV}$ ) is reached by the scaler mode technique, in which the total counting rates of each cluster are recorded every 500 ms, with no information on the arrival direction and spatial distribution of the detected particles. Four low multiplicities channels in each cluster are implemented for event multiplicities from  $\geq 1$  to  $\geq 4$ . The measured counting rates are respectively  $\sim 40 \text{ KHz}$ ,  $\sim 2 \text{ KHz}$ ,  $\sim 300 \text{ Hz}$  and  $\sim 120 \text{ Hz}$ . The counting rate for a given multiplicity is obtained using the following relation:  $n_i = n_{\geq i} - n_{\geq i+1}$ , where  $n_i$  is the counting rate for the  $i_{th}$  multiplicity.

Dealing with transient phenomena, it is important to understand the detector statistical behaviour. For each Cluster, we studied the counting rate distribution for each multiplicity. As shown in figure 1a, the exact multiplicity counting rate follows a Poissonian distribution, while the total counting rate added up on the 4 multiplicities channels (figure 1b) follows, due to correlation between different scalers, a distribution which is larger than a Poissonian distribution, with a  $\sigma^2$  given by the following expression:

$$\sigma^2(n_{tot}) = \sigma^2(n_1) + 4\sigma^2(n_2) + 9\sigma^2(n_3) + 16\sigma^2(n_4).$$

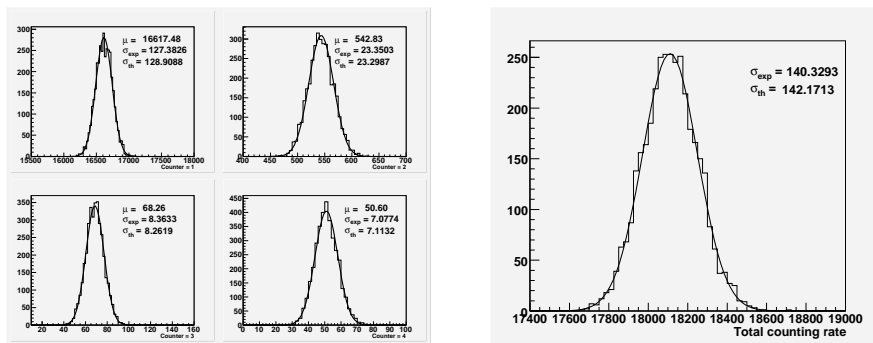


Fig. 1. a. Counting distribution for each multiplicity over a period of 30 minutes for a typical cluster; b. Total counting rate summed over the multiplicities channels for the same cluster.

In order to estimate the sensitivity of the detector, the effective area of the complete detector has been calculated for each multiplicity with a MonteCarlo simulation for photons and protons in the energy range between 1GeV and 1TeV and at zenith angle  $\theta = 0^\circ, 10^\circ, 20^\circ, 40^\circ$  (see figure 2). For multiplicity  $n = 1$  the detector sensitivity does not depend on its geometrical features and the effective areas for any carpet dimension can be scaled from the plotted values [3].

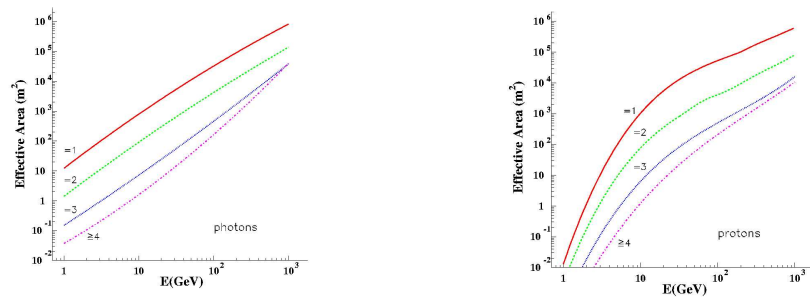


Fig. 2. Effective areas for primary photons (left plot) and protons (right plot) with zenith angle  $\theta = 20^\circ$ . The curves refer to different multiplicity channels:  $n = 1$ ,  $n = 2$ ,  $n = 3$  and  $n \geq 4$ .

### 3. Search for high energy emission from GRB in coincidence with satellite

Following the first GRB detection by Swift on December 17, 2004, a search has been conducted for an excess in the counting rate of the single multiplicity channel during the time duration  $\Delta t_{90}$  measured by the satellites, estimating the background from the average counting rate in a time window 20 times the  $\Delta t_{90}$ . Up to May 2006, 28 GRBs detected by satellites were within  $\theta \leq 40^\circ$ , but due to the detector installation and debugging operations, reliable data are available only for 16 of them. For each GRB the excess of the signal in units of standard deviations has been calculated and it is shown in column 8 in table 1. In particular three GRBs (GRB05114, GRB060105 and GRB060510A) show a statistical significance equal to 2.8, 3.6 and 3.7 respectively. Taking into account that we considered a sample of 16 GRBs, these values correspond to a post-trial probability of  $1.7\sigma$ ,  $2.8\sigma$  and  $2.9\sigma$  respectively. For none of these 16 GRBs a significant excess has

been observed in the burst time window and  $3\sigma$  fluence upper limits were set in the energy range 1 - 100 GeV using the spectral index measured by the satellites. For GRBs with known redshift, the upper limit was calculated assuming the  $\gamma\gamma$  absorption model of Kneiske et al [4].

Table 1. List of GRBs searched by ARGO-YBJ with preliminary upper limits

GRB	Instrum.	T90 (s)	$\theta$ (deg)	Redshift	Spectral Index	Carpet Area (m <sup>2</sup> )	$\sigma$	Fluence UL (erg/cm <sup>2</sup> )
041228	Swift	62	28.1	-	1.56	693	-1.3	$3.3 \cdot 10^{-4}$
050408	HETE	15	20.4	1.24	1.98	1820	-2.2	$9.6 \cdot 10^{-5}$
050509A	Swift	12	34.0	-	2.1	1820	0.29	$1.6 \cdot 10^{-4}$
050528	Swift	11	37.8	-	2.3	1820	-0.012	$6.5 \cdot 10^{-4}$
050802	Swift	20	22.5	1.71	1.55	1820	0.74	$1.0 \cdot 10^{-4}$
051022	HETE	200	37.9	0.8	1.22	3379	-0.68	$9.8 \cdot 10^{-4}$
051105A	Swift	0.3	28.5	-	1.33	3379	0.90	$1.4 \cdot 10^{-5}$
051114	Swift	2	32.8	-	1.22	3379	2.8	$1.9 \cdot 10^{-5}$
051227	Swift	8	22.8	-	1.31	3379	0.93	$2.5 \cdot 10^{-5}$
060105	Swift	55	16.3	-	1.11	3379	3.6	$5.9 \cdot 10^{-5}$
060111	Swift	13	10.8	-	1.63	3379	0.82	$2.5 \cdot 10^{-5}$
060115	Swift	142	16.6	3.53	1.76	4505	-2.2	$2.3 \cdot 10^{-4}$
060421	Swift	11	39.3	-	1.53	4505	-0.46	$1.6 \cdot 10^{-4}$
060424	Swift	37	6.7	-	1.72	4505	1.9	$4.1 \cdot 10^{-5}$
060427	Swift	64	32.6	-	1.87	4505	-1.8	$1.8 \cdot 10^{-4}$
060510A	Swift	21	37.4	-	1.55	4505	3.7	$2.3 \cdot 10^{-4}$
060526	Swift	14	31.7	3.21	1.66	4505	0.75	$1.2 \cdot 10^{-4}$

#### 4. Conclusion

The ARGO-YBJ detector installation is almost completed and the detector is already in data taking, showing the expected statistical behaviour. Until now, the search for high energy emission from GRBs has given no positive result. The scaler mode has already shown a good sensitivity, with fluence upper limits  $\sim 10^{-4} - 10^{-5}$  erg/cm<sup>2</sup> in the energy range between 1 - 100 GeV.

#### References

1. J.R. Catelli et al., AIP Conf. Proc. No.428, p.309 (AIP New York 1998).
2. 29th ICRC Pune, India (August 3 - August 10, 2005).
3. S. Vernetto, Astrop. Phys. 13 (2000) 75.
4. T.M. Kneiske et al. A&A 413 (2004) 807.